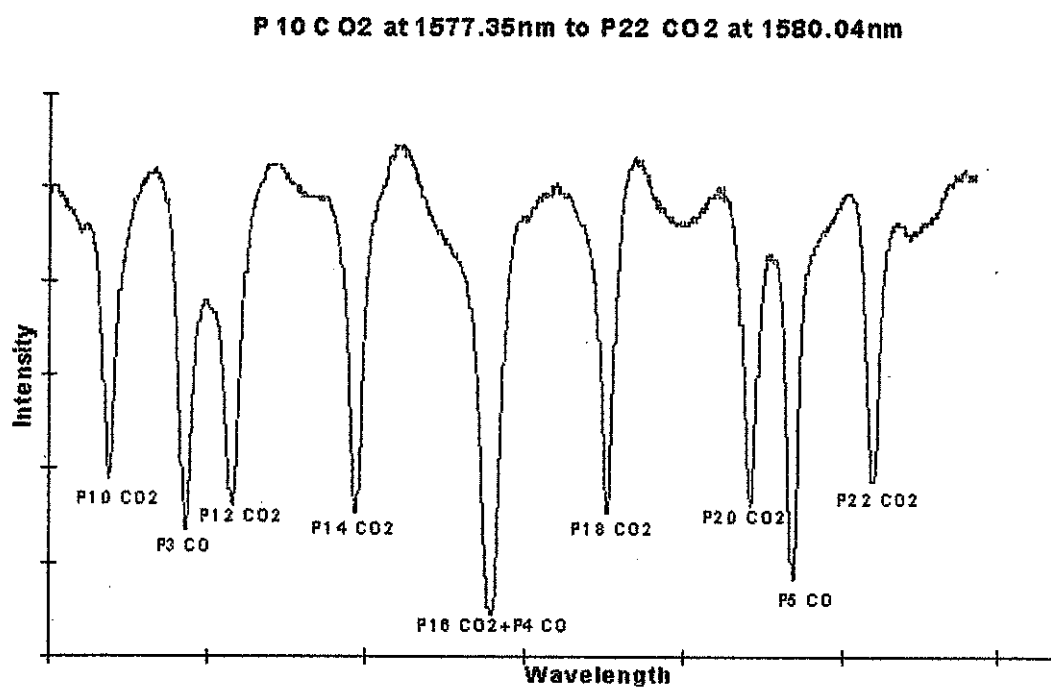


# Absorption Spectroscopy of Carbon Monoxide in a Mixture of Carbon Dioxide



# Absorption Spectroscopy of Carbon Monoxide in a Mixture of Carbon Dioxide

## **Abstract**

### **Absorption Spectroscopy of Carbon Monoxide in a Mixture of Carbon Dioxide**

Absorption spectroscopy in the infrared region has been compared to absorption spectroscopy in the microwave region theoretically with respect to which useful areas they can be used. Experiments have also been performed where a tuneable diode laser was used to measure the 3-0 band of carbon monoxide in a mixture of carbon dioxide. Several spectra were obtained and the absorption lines were identified, both for carbon monoxide and carbon dioxide. Most of the work concentrated on the R-13 line, located at 1564.16 nm, and the R-14 line, located at 1563.61 nm, in carbon monoxide. The measurements were performed at two different pressures, 1 atmosphere and 10 mbar. The line profile at 10 mbar is explained with the Doppler function and was coinciding almost exactly. In the 1 atmosphere measurement, the line profile should be dominated by collision broadening but was almost twice as broad as the theoretical collision profile for the same pressure. This is explained by the presence of carbon dioxide. The origin of a periodic noise is also explained and is used to show how well the laser used work.

Key words:

**SP Sveriges Provnings- och  
Forskningsinstitut**  
SP Rapport 2001:25  
ISBN 91-7848-869-9  
ISSN 0284-5172  
Borås 2001

**SP Swedish National Testing and  
Research Institute**  
SP Report 2001:25

Postal address:  
Box 857, SE-501 15 BORÅS, Sweden  
Telephone: +46 33 16 50 00  
Facsimile: +46 33 13 55 02  
E-mail: [info@sp.se](mailto:info@sp.se)  
Internet: [www.sp.se](http://www.sp.se)

# Contents

<b>Abstract</b>	<b>2</b>
<b>Contents</b>	<b>3</b>
<b>Acknowledgements</b>	<b>4</b>
<b>1 Introduction</b>	<b>5</b>
<b>2 Theory of Molecular Structure</b>	<b>6</b>
2.1 Introduction	6
2.2 Electronic Transitions	7
2.3 Rotation Transitions	7
2.4 Vibration Transitions	8
2.5 Microwave Spectroscopy of Diatomic Molecules	9
2.6 Infrared Spectroscopy of Diatomic Molecules	12
2.7 The Diatomic Vibrating-Rotator	15
2.8 Line Broadening Effects	15
2.8.1 Natural Broadening	16
2.8.2 Doppler Broadening	16
2.8.3 Collision Broadening	17
<b>3 Detection Sensitivity in Molecular Spectroscopy</b>	<b>18</b>
3.1 Frequency Modulation	18
3.2 Sensitivity in Absorption Techniques	18
3.3 Limits	18
<b>4 Experiment and Methods</b>	<b>20</b>
4.1 Experimental Setup	20
4.2 Results	20
<b>5 Optical or Sub-mm Spectroscopy?</b>	<b>28</b>
5.1 Broadening and Spectral Resolution	28
5.2 Absorption Strength	28
5.3 Water and Other Limiting Effects	30
<b>6 Conclusion and Future Work</b>	<b>32</b>
<b>References</b>	<b>33</b>
<b>APPENDICES</b>	<b>34</b>

# Acknowledgements

This work was performed as a master thesis in physics at Göteborg University. Project partners were the Swedish National Testing and Research Institute (SP), Department of Microelectronics and Nano Science at Chalmers University of Technology. The practical work was performed at SP. The author is grateful to Leslie Pendrill at SP for good supervision and guiding, Anne Andersson-Fäldt at SP for comments and laboratory space, Ivanov Zdravko at CTH for letting me use equipment and given me an introduction to Josephson spectroscopy, and Jonas Bengtsson for his help with the computer when writing the report.

# 1 Introduction

Spectroscopic techniques can work well without preconditioning of the gas [Linnerud 1998]. They therefore have the potential of *in-situ* measurements with fast response and are ideally suited for industrial applications provided they could measure with sufficient sensitivity.

A number of spectroscopic techniques have been developed for trace gas measurements. The now traditional technique has been non-dispersive infrared spectroscopy where the transmission has been measured at two wavelengths, one absorbing and the other at non-absorbing. This technique is suited for gases with broad absorption bands. In recent years new techniques have emerged such as Fourier transform infrared, different optical absorption spectroscopy, laser induced fluorescence and tuneable diode laser absorption spectroscopy, which was used in this work.

This work consists of two parts. First microwave spectroscopy of molecules is compared with infrared spectroscopy theoretically. Second a method of absorption spectroscopy in the infrared region of carbon monoxide is presented and discussed.

The middle infrared,  $3\mu\text{m} - 15\mu\text{m}$ , is a very rich spectral region where most of the interesting trace gases absorb on their fundamental rotation/vibration modes. The absorption is so strong, particularly from  $\text{H}_2\text{O}$  and  $\text{CO}_2$  molecules, that a very high spectral resolution is required to avoid interference between species. Tuneable diode lasers have line widths of only a few MHz or less and are therefore well suited for high-resolution spectroscopy. In the near infrared,  $0.8\mu\text{m} - 3\mu\text{m}$ , we have the first and second overtones of the rotation/vibration modes of the trace gases, and there are commercial semiconductor lasers available up to approximately  $2\mu\text{m}$  that operate at room temperature. The transitions studied in this work were from the ground state to the second overtone. Due to weak absorption, the sensitivity had to be increased. An easy way to increase sensitivity is to increase the optical path length, which can be extended with multipath cells, as done in this work.

In the practical absorption spectroscopy experiment, carbon monoxide was chosen. For reasons of convenience a mixture was used. The mixture consisted of 40 % carbon monoxide and 60 % carbon dioxide.

Highly accurate rotational transition frequencies of CO have always been in demand since they serve in the laboratory as an easy but important secondary calibration standard, covering the millimetre to the far infrared region. This means that exact references are available for applications for instance in optical communication. Astrophysical, CO is an interstellar molecule, and an important trace constituent of planetary atmospheres. For both cases, precise laboratory rest frequencies are required for accurate velocity determinations [Winnewisser 1997].

There has been increasing concern about man made pollution in the atmosphere over the last few decades. The dilution of pollutants in the atmosphere makes the concentration very low, often below 1 ppb [Linnerud 1998] and therefore difficult to measure. Measurement of some gases such as CO and  $\text{NO}_x$  is done routinely in many cities.

First the theory of molecular structure is described in order to point out the differences between rotation and vibration in molecules. Then different broadening effects are discussed. Last the theory is used to explain our practical results.

## 2 Theory of Molecular Structure

### 2.1 Introduction

In classical absorption spectroscopy, radiation sources with a broad emission continuum are used. The radiation is collimated and passes through the absorption cell. Behind a dispersing instrument for wavelength selection the intensity  $I(\lambda)$  of the transmitted light is measured as a function of the wavelength  $\lambda$  (see figure 1).

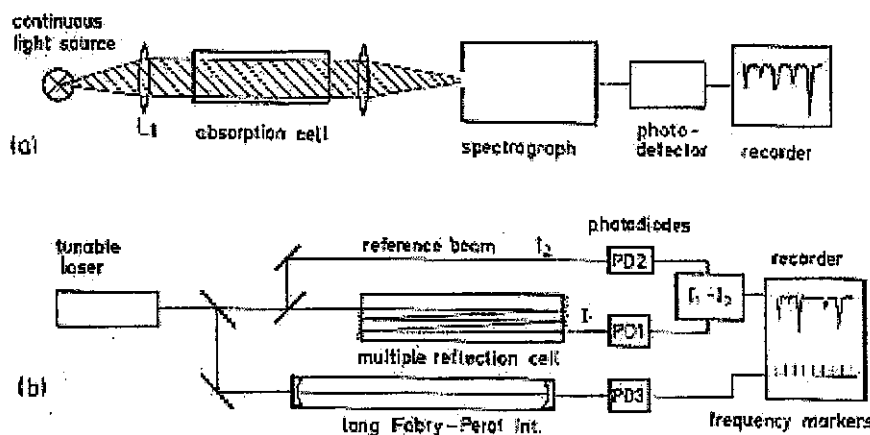


Figure 1: Comparison between absorption spectroscopy with broadband incoherent source (a) and with tuneable single-mode laser (b). Figure taken from Demtröder [ 1981].

The spectral resolution is generally limited by the resolving power of the dispersing spectrometer. Only with large and expensive instruments (e.g. Fourier spectrometers) may the Doppler limit be reached (see Line Broadening Effects). The detection sensitivity of the experimental arrangement is defined by the minimum absorbed power that can still be detected. In most cases it is limited by detector noise and by intensity fluctuations of the radiation source.

Contrary to radiation sources with broad emission continua used in conventional spectroscopy, tuneable lasers offer radiation sources in the spectral range from the UV to the IR with extremely narrow bandwidths and with spectral power densities which may exceed these of incoherent light sources by many orders of magnitude [Demtröder 1981]. The advantages of absorption spectroscopy with tuneable lasers may be summarized as follows.

No monochromator is needed. The spectral resolution is higher. With tuneable single mode lasers it is limited only by the line widths of the absorbing molecular transitions. Using Doppler free techniques even sub Doppler resolution can be achieved.

Because of the high spectral power density of many lasers, detector noise is generally negligible. Intensity fluctuations of the laser, which limit the detection sensitivity, may be essentially suppressed by intensity stabilization. This furthermore increases the signal to noise ratio.

Because of the good collimation of a laser beam, long absorption paths can be realized by multiple reflections back and forth through the absorption cell. Such long absorption paths enable the measurement of transitions even with small absorption coefficients. Furthermore using low gas pressure can reduce pressure broadening. This is especially important in the infrared region (or microwave) where Doppler widths are small and the pressure broadening become the limiting factor for the spectral resolution (see 2.8 Line Broadening Effects).

The development of semiconductor lasers in the near infrared has been spurred by the development of CD players ( $0.78\mu\text{m}$ ) and fibre optic communication ( $1.3\mu\text{m}, 1.55\mu\text{m}$ ). As technology has improved, lasers have been developed for new applications such as pumping of solid state ( $0.808\mu\text{m}$ ) and fibre ( $0.98\mu\text{m}$ ) lasers [Linnerud 1998].

In addition to wavelength, other important laser parameters are mode stability, in order to obtain single frequency operation, current tune ability, and frequency drift. Fabry-Perot type lasers are unreliable with respect to mode jumping. Therefore other types of semiconductor lasers such as distributed feedback, distributed Bragg reflector and vertical cavity surface emitting lasers have been developed.

## 2.2 Electronic Transitions

An electron transition is a transition between two electronic states. These states are often separated by significant differences in energy. The result of this is that most of the transitions are caused by energies in the range of 1 to 10 eV.

## 2.3 Rotation Transitions

A molecule such as carbon monoxide, CO, in which one atom (the carbon) carries a permanent net positive charge and the other a net negative charge, is said to have a permanent electric dipole moment. O<sub>2</sub> on the other hand, in which there is no such charge separation, have a zero dipole. If we consider the rotation of CO, we see that the plus and the minus charges change place periodically, and the component of dipole moment in a given direction fluctuates regularly.

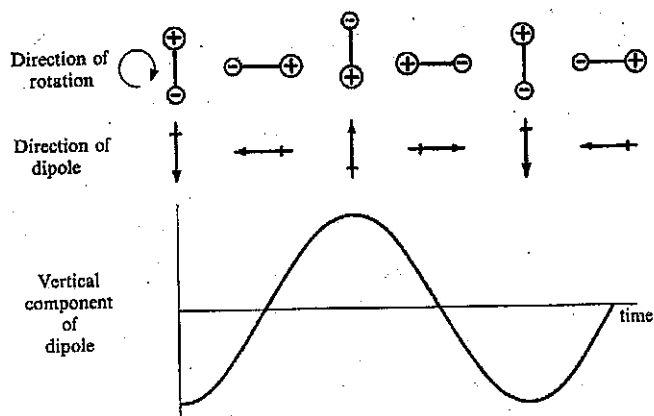
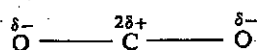


Figure 2: The dipole moment changes periodically for a rotating heteronuclear molecule.

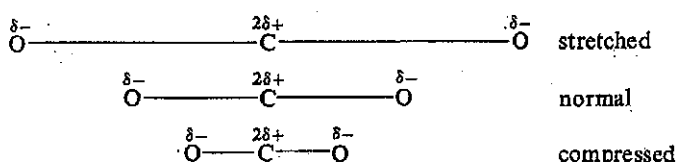
This fluctuation is plotted in the lower half of figure 2, and it is seen to have same form as a fluctuating electric field of radiation [Banwell 1972]. Thus if interaction between the molecule and electronic radiation occur, energy can be absorbed or emitted, and the rotation gives rise to a spectrum. If there is no dipole, as in CO<sub>2</sub>, no interaction can take place and the molecule is microwave inactive. This imposes a limitation of the application of microwave spectroscopy. Rotational transitions are caused by wavelengths between 15 μm and 1 cm.

## 2.4 Vibration Transitions

Here it is vibration, which give rise to a dipole change. Consider the carbon dioxide molecule (which does not have microwave spectra due to the non-dipole structure), in which the atoms are arranged linearly with a small positive net charge on the carbon and small negative charges on the oxygen.



During the mode of vibration known as the symmetric stretch, the molecule is alternately stretched and compressed, both bonds changing simultaneously.



The dipole moment remains zero throughout the whole of this motion, and this motion is infrared inactive. There is another stretching vibration called anti symmetrical stretch (see figure 3).

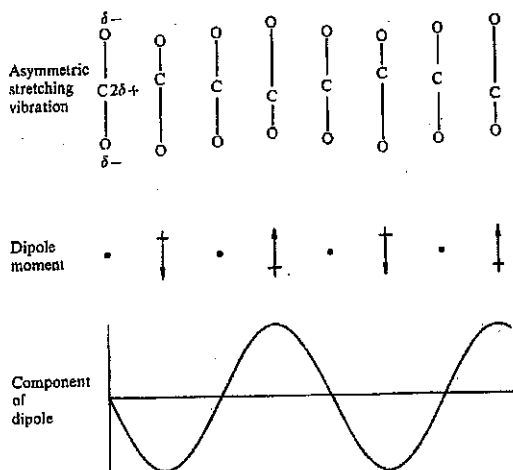


Figure 3: Anti-symmetrical stretch of carbon dioxide.

Here one bond stretches while the other is compressed, and vice versa. There is a periodic alteration in the dipole moment, and the vibration is thus infrared active. One further vibration is allowed to this molecule, known as the bonding mode (see figure 4).

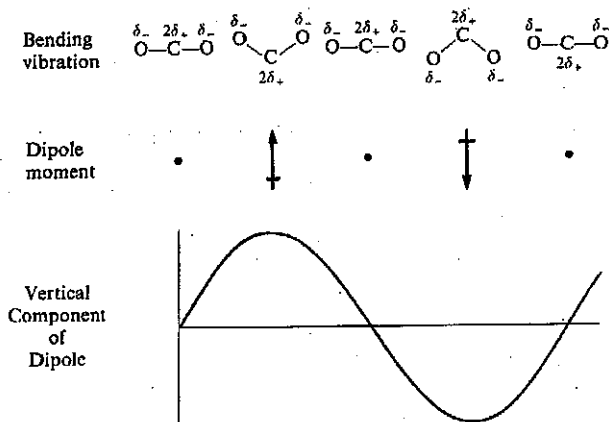


Figure 4: Bonding mode of carbon dioxide.

This is also infrared active. In both these motions the centre of gravity does not move. Vibration transitions are caused by wavelengths between 1 and  $100\mu\text{m}$ .

## 2.5 Microwave Spectroscopy of Diatomic Molecules

By use of the Schrödinger equation [Barone 1972] it may be shown that the rotational energy levels allowed to the rigid diatomic molecule are given by

$$E_J = \frac{h^2}{8\pi^2 I} J(J+1) \text{ Joules, where } J = 0, 1, 2, \quad (1)$$

$h$  is the Planck constant, and  $I$  is the moment of inertia. The quantity  $J$ , which can take integral values from zero upwards, is called the rotational quantum number; its restriction to integral values arises directly out of the solution to the Schrödinger equation, and it is this restriction, which effectively allows only certain discrete rotational energy levels in the molecule. Equation (1) is usually written as

$$\epsilon_J = BJ(J+1) \text{ cm}^{-1}, J = 0, 1, 2, \dots$$

where  $B$ , the rotational constant, is given by

$$B = \frac{h}{8\pi^2 Ic} \text{ cm}^{-1}.$$

If one wants to discuss the spectrum, one needs to consider the differences between the levels. Consider the molecule to be in the  $J=0$  (the ground rotational state, in which no rotation occurs), and let incident radiation be absorbed to raise it to the  $J=1$  state. The energy absorbed will be

$$\varepsilon_{J=1} - \varepsilon_{J=0} = 2B - 0 = 2B \text{ cm}^{-1}.$$

If now the molecule is raised from the  $J=1$  to the  $J=2$  level by the absorption of more energy

$$\varepsilon_{J=2} - \varepsilon_{J=1} = 6B - 2B = 4B \text{ cm}^{-1}.$$

In deriving this pattern we have made the assumption that a transition can occur from a particular level only to its immediate neighbour, either above or below. In fact, an application of the Schrödinger wave equation shows that. So, the only transitions that have to be considered is when  $J$  changes by one unit. All other transitions are spectroscopically forbidden.

$$\Delta J = \pm 1.$$

If  $\Delta J = -1$  it is usually called the P-branch and if  $\Delta J = +1$  it is referred to as the R-branch.

The Schrödinger equation may be set up for a non-rigid molecule, and the rotational energy levels are found to be [Gordy 1984]

$$\varepsilon_J = \frac{E_J}{hc} = BJ(J+1) - DJ^2(J+1)^2 \text{ cm}^{-1}, \quad (2)$$

where rotational constant,  $B$ , is defined above, and the centrifugal distortion constant,  $D$ , is given by

$$D = \frac{h^3}{32\pi^4 I^2 r^2 kc} \text{ cm}^{-1}$$

which is a positive quantity.  $k$ , the force constant, is  $k = 4\pi^2 \omega^2 c^2 \mu$  and  $r$  is inter nuclear distance. Equation (2) applies for a simple harmonic force field only. If the force field is un-harmonic, the expression becomes

$$\varepsilon_J = B(J+1) - DJ^2(J+1)^2 + HJ^3(J+1)^3 + KJ^4(J+1)^4 \dots \text{ cm}^{-1},$$

where  $H$ ,  $K$ , etc., are small constants dependent upon the geometry of the molecule. They are, however, negligible compared with  $D$ .

From the defining of  $B$  and  $D$  it may be shown that

$$D = \frac{16B^3\pi^2\mu c^2}{k} = \frac{4B^3}{\omega^2}$$

where  $\omega$  is the vibration frequency of the bond.

Vibration frequencies are usually in the order of  $10^3 \text{ cm}^{-1}$ , while  $B$  is in order of  $10 \text{ cm}^{-1}$ . Thus  $D$ , being of the order of  $10^{-3} \text{ cm}^{-1}$  and very small compared with  $B$ . For small  $J$  the correction term  $DJ^2(J+1)^2$  is almost negligible, while for  $J$  values of 10 or more it may become appreciable.

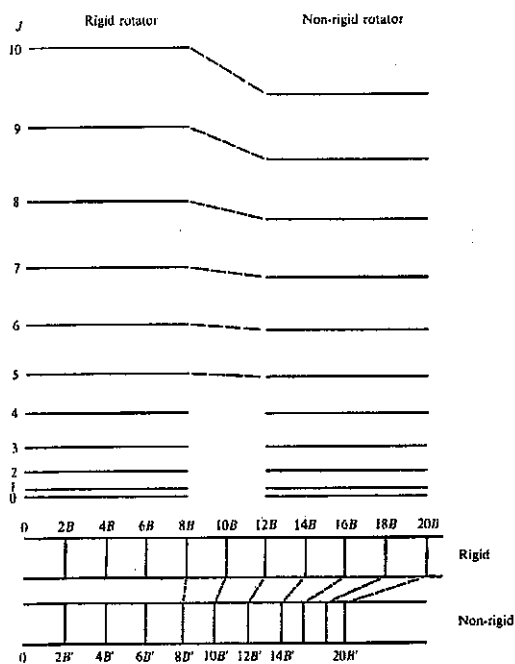


Figure 5: The change in rotational levels and rotational spectrum when passing from a rigid to a non-rigid diatomic molecule. Figure taken from Banwell [1972].

Figure 5 shows, much exaggerated, the lowering of rotational levels when passing from the rigid to the non-rigid diatomic molecule. The spectra are also compared, the dotted lines connecting corresponding energy levels and transitions of the rigid and non-rigid molecules.

## 2.6 Infrared Spectroscopy of Diatomic Molecules

If one approximates the molecule by two masses attached together with a spring that obeys Hooke's law, one has the simple harmonic vibration approximation. The potential energy of the molecule follows a simple parabola, as seen in figure 6.

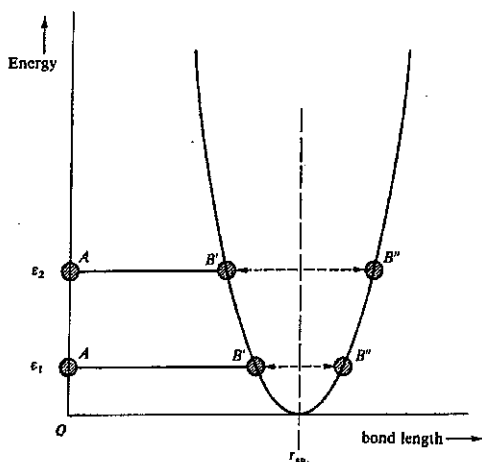


Figure 6: Parabolic curve of energy plotted against the extension or compression of a spring obeying Hooke's law. Classically, the energy levels are found to be

$$\epsilon_v = \frac{E_v}{hc} = \left(v + \frac{1}{2}\right) \overline{\omega}_{osc.} \text{ cm}^{-1}.$$

These are the only allowed energies for the simple harmonic vibrator. One should notice that the lowest vibration energy, obtained by putting  $v = 0$  is  $\epsilon_0 = \frac{1}{2} \overline{\omega}_{osc.} \text{ cm}^{-1}$ . The

implication is that a molecule can never have zero vibration energy. The quantity  $\frac{1}{2} \overline{\omega}_{osc.}$  is known as the zero-point energy, this only due to the classical frequency and hence on the strength of the chemical bond and the atomic masses.

The selection rule for the harmonic oscillator undergoing vibration changes [Gordy 1984]

$$\Delta v = \pm 1$$

Real molecules do not obey exactly the laws on simple harmonic motion; real bonds are not so homogeneous as they obey Hooke's law. If the bond between atoms are stretched, there comes a point at which it will brake. For small compression and extensions the bond may be taken as perfectly elastic. For larger amplitudes much more complicated behaviour must be assumed. Figure 7 shows the shape of the energy curve for a typical diatomic molecule, together with the ideal, simple harmonic parabola.

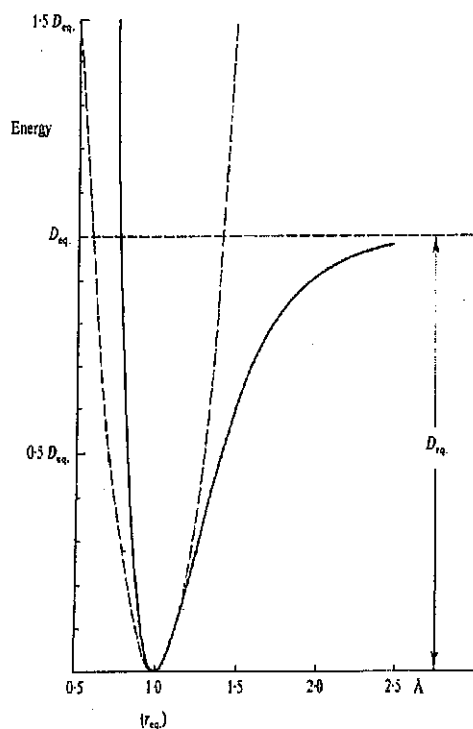


Figure 7: The Morse curve: the energy of a diatomic molecule undergoing un-harmonic extension and compressions. Figure taken from Banwell [1972].

An empirical expression which fits this curve was derived by P.M. Morse, and is called the Morse function

$$E = D_{eq} \left[ 1 - e^{a(r_{eq}-r)} \right]^2, \quad (3)$$

where  $a$  is a constant for a particular molecule and  $D_{eq}$  is the dissociation energy. When equation (3) is used in the Schrödinger equation, the pattern of the allowed vibration energy levels is found to be

$$\epsilon_v = (v + \frac{1}{2})\bar{\omega}_e - (v + \frac{1}{2})^2 \bar{\omega}_e \chi_e \text{ cm}^{-1} \quad v = 0, 1, 2, \dots \quad (4)$$

where  $\bar{\omega}_e$  is an oscillation frequency (expressed in wave numbers) and  $\chi_e$  is the corresponding anharmonicity constant which, for bond stretching vibrations, is always small and positive, so that the vibration levels crowd more closely together with increasing  $v$ , (see figure 8).

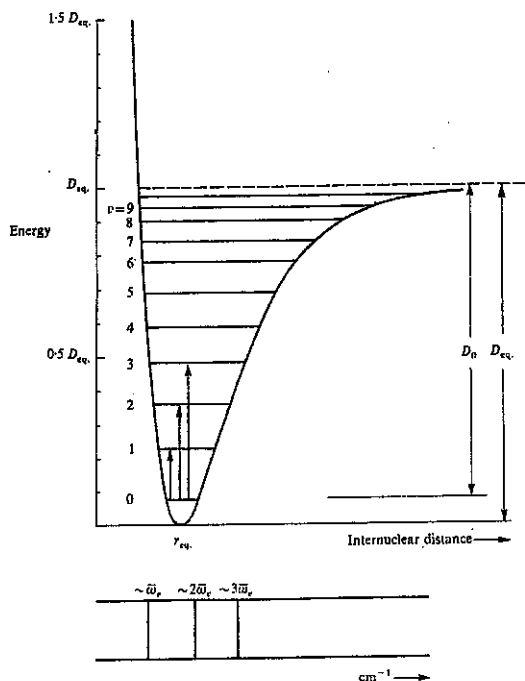


Figure 8: The allowed vibration energy levels and some transitions between them for a diatomic molecule undergoing anharmonic oscillations. Figure taken from Banwell [1972].

The selection rules for the anharmonic oscillator are found to be

$$\Delta v = \pm 1, \pm 2, \dots$$

Thus they are the same as for the harmonic oscillator, with the additional possibility of larger jumps. These, however, are predicted by theory and observed in practice to be of rapidly diminishing probability. To a good approximation, since  $\chi_e$  are very small, the three spectral lines lie very close to  $\omega_e$ ,  $2\omega_e$  and  $3\omega_e$ . The line near  $\omega_e$  is called the fundamental absorption, while those near  $2\omega_e$  and  $3\omega_e$  is called the first and second overtones, respectively.

## 2.7 The Diatomic Vibrating-Rotator

A typical diatomic molecule has rotational energy separations of 1-10  $\text{cm}^{-1}$ , while the vibration energy separations is in order of  $10^3 \text{ cm}^{-1}$ . Since the energies of the two motions are so different we may consider that a diatomic molecule can execute rotations and vibrations independently. This is called the Born-Oppenheimer approximation. The approximation is to assume that the combined rotation-vibration energy is simply the sum of the separate energies

$$\epsilon_{total} = \epsilon_{rot.} + \epsilon_{vib.} \text{ (cm}^{-1}\text{)}.$$

Note that since the rotational constant in the equation above is taken to be the same for all  $J$  and  $v$  (a consequence of the Born-Oppenheimer approximation), the separation between two levels of given  $J$  is the same in the  $v = 0$  and  $v = 1$  states. It may be shown that the selection rules for the combined motions are the same as those for each separately

$$\Delta v = \pm 1, \pm 2, \text{ etc.} \quad \Delta J = \pm 1.$$

Note that a diatomic molecule, except under very special and rare circumstances, may not have  $\Delta J = 0$ , in other words a vibration change must be accompanied by a simultaneous rotational change.

## 2.8 Line Broadening Effects

Spectral lines in discrete absorption or emission spectra are never strictly monochromatic. One always observes a spectral distribution  $I(\nu)$  of the absorbed or emitted intensity around the central frequency  $\nu_0 = (E_i - E_k)/h$  corresponding to a molecular transition with the energy difference  $\Delta E = E_i - E_k$  between upper and lower level. The function  $I(\nu)$  in the vicinity of  $\nu_0$  is called the line profile (*see* figure 9). The frequency interval  $\delta\nu = |\nu_2 - \nu_1|$  between the two frequencies  $\nu_1$  and  $\nu_2$  for which  $I(\nu_1) = I(\nu_2) = I(\nu_0)/2$  is the full width at half maximum of the line (FWHM), often shortly called the line width or half width of the spectral line.

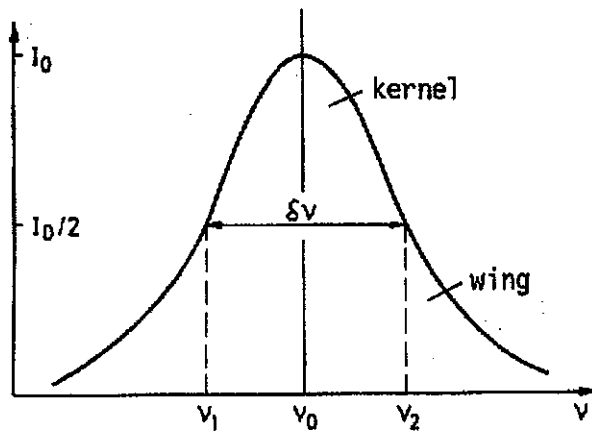


Figure 9: Line profile, half width, kernel and wings of a spectral line.

In order to avoid  $2\pi$  in the equations the angular frequency  $\omega = 2\pi\nu$  is often used. There are three contributions to the line width of an absorption line: natural line broadening, Doppler broadening and collision broadening. In most industrial processes collision broadening dominates which, in the impact approximation, results in a Lorentzian line shape. For a more precise line shape one has to combine the effects of Doppler broadening and collision broadening which gives a Voigt line shape [Henningesen 1999]. Pressure and temperature therefore strongly influence the line width.

### 2.8.1 Natural Broadening

By looking at the molecule as vibrating system, with a damping term  $\gamma$ . This damping term is the inverse of the lifetime of the excited energy state. The line profile becomes

$$g(\omega - \omega_0) = \frac{1}{2\pi} \frac{\gamma}{(\omega - \omega_0)^2 + (\gamma/2)^2}, \quad [\text{Demtröder 1981}]$$

where  $\omega_0$  is the line centre frequency.  $g(\omega - \omega_0)$  are called the normalized Lorentzian profile. Its full width becomes

$$\delta\omega_n = \gamma$$

### 2.8.2 Doppler Broadening

Generally the Lorentzian line profile with the natural line width, as discussed above, cannot be observed without special techniques, because it is completely concealed by other broadening effects. One of the major contributions to the spectral line width in gases at low pressures is the Doppler width, which is due to thermal motion of the absorbing or emitting molecules.

The intensity profile of a Doppler broadened spectral line becomes

$$I(\omega) = I_0 \exp\left(-\frac{c(\omega - \omega_0)^2}{\omega_0 v_p}\right), \quad [\text{Demtröder 1981}]$$

where  $I_0$  is the intensity without absorption,  $\omega_0$  is the line centre frequency and  $v_p$  is the most probably velocity of the molecules.

This Gaussian profile with a half width  $\delta\omega_D = |\omega_1 - \omega_2|$  with  $I(\omega_1) = I(\omega_2) = I(\omega_0)/2$ ,

$$\delta\omega_D = \frac{\omega_0}{c} \sqrt{\frac{8kT \ln 2}{m}}$$

This quantity is called the Doppler width. Note that  $\delta\omega_D$  increases linearly with frequency  $\omega_0$ , so one should expect smaller Doppler width for microwave transitions than for transitions in the infrared.

### 2.8.3 Collision Broadening

When a molecule  $A$  with energy levels  $E_i$  and  $E_k$  approaches another molecule  $B$ , the energy levels of  $A$  are shifted because of the interaction between  $A$  and  $B$ . This shift depends on the electron configuration of  $A$  and  $B$  and on the distance  $R(A,B)$  between both collision partners, which could be defined as the distance between the centres of mass between  $A$  and  $B$ . During a collision, the lifetime of the molecule in an excited state may be shortened compared with the natural/radiative lifetime.

Both of these pressure dependent effects can cause a corresponding pressure dependent line width  $\delta\omega$  which is proportional to the pressure  $p$  of the collision partners and which can be described by a sum of two damping terms

$$\delta\omega = \delta\omega_n + \delta\omega_{col}$$

The collision induced additional line broadening is therefore often called pressure broadening.

Collision broadening depends not only on pressure but also on the collision cross section of the molecules. Variations in gas composition may therefore influence the line width, as can be seen in 4.2 Results.

### 3 Detection Sensitivity in Molecular Spectroscopy

Detection of absorption by molecular samples can be made more sensitive in two ways, either the absorption signal is enhanced or the background noise is reduced. The absorption signal is simply enhanced by placing a cavity around the sample in order to increase the effective cell length. The ultimate detection sensitivity is achieved when each absorption event is observed and the noise basically limited by the uncertainty of event occurrence.

#### 3.1 Frequency Modulation

The most straightforward measurement principle is direct absorption measurement where the absorption at the line centre is compared with the absorption slightly at the side of the line. In its simplest form this technique is not used much because measuring the difference between two large signals gives rather low detection sensitivity. To improve this, a modulation of the laser frequency is applied. The instantaneous laser frequency is then

$$f(t) = f_0 + m\gamma \sin(2\pi f_m t)$$

where  $f_0$  is the centre laser frequency,  $\gamma$  is the half width at half maximum of the absorption line,  $f_m$  is the modulation frequency and  $m$  is the frequency modulation index. If  $f_m \ll \gamma$  this is referred to as wavelength modulation spectroscopy, otherwise it is called frequency modulation spectroscopy [Linnerud 1998].

The frequency modulation in the microwave region is not that different from the optical region.

#### 3.2 Sensitivity in Absorption Techniques

All absorption spectroscopy is based on the Beer-Lambert law, which states that the transmission will decay exponentially. For sufficiently low pressures (less than a few bar) many gases will have distinct absorption lines of width in the order of  $0.01$  to  $0.1 \text{ cm}^{-1}$  depending on pressure and other broadening effects.

To avoid low frequency noise of technical origins, signal detection should compare on resonant and off resonant cases in quick successions. By simultaneously obtaining and subtracting these cases, one provides a signal with no output unless there is a resonance. This is accomplished by use of the frequency modulation technique.

#### 3.3 Limits

In the optical region the detection sensitivity are limited by the bandwidth of the detector. Low frequency noise, which has its origin in technical apparatus, also becomes a limiting factor, but can be reduced by modulation techniques.

In sub-mm spectroscopy, it is the detector or the radiation source that decides which signal to noise ratio that can be achieved.

One of the most sensitive detectors is a detector that uses a SIS junction (Superconductive layer, Insulator layer, and Superconductive layer). The SIS junction is often used in heterodyne detection mode. The principle of a heterodyne detector is that it mixes a weak incoming signal with a strong local oscillator signal and generates a signal at the difference frequency. Mixing occurs whenever radiation of two different frequencies is impinging on a device, which has a non-linear current voltage characteristic. This is the case for SIS junctions [de Lange 1994]. An advantage of heterodyne mixing as compared to direct detection is that the spectral information at a high frequency signal is converted to a much lower frequency.

In order to reduce the detector noise the detector can be cooled; this of course reduces the thermal noise. Winnewisser [1997] says that in their experiment, the limit on the signal to noise ratio, was the output signal from the KVARZ synthesizer, which was used as a local oscillator.

Even though they say that the signal to noise ratio can be better they determined the line position in the sub-mm region with an accuracy better than 500Hz and Belov [1995] 5kHz. Winnewisser [1997] used sub-Doppler techniques and got a line width of only 40kHz. In the optical region Picqué [1997] were able to determine the line position with an accuracy of 1MHz.

Further discussion of the absorption sensitivity of different spectroscopic methods will be deferred to section 5.2.

## 4 Experiment and Methods

The experimental part of this work consists of a study of the transition from the vibration ground state ( $v = 0$ ) to the second overtone ( $v = 3$ ). Because of the weak absorption in the 3-0 band of carbon monoxide, a multipath cell is used to increase the absorption length of the sample. The method used in the optical area is described by figure 10. This work is concentrated on the R-branch and the R14- and R13-line specially.

### 4.1 Experimental Setup

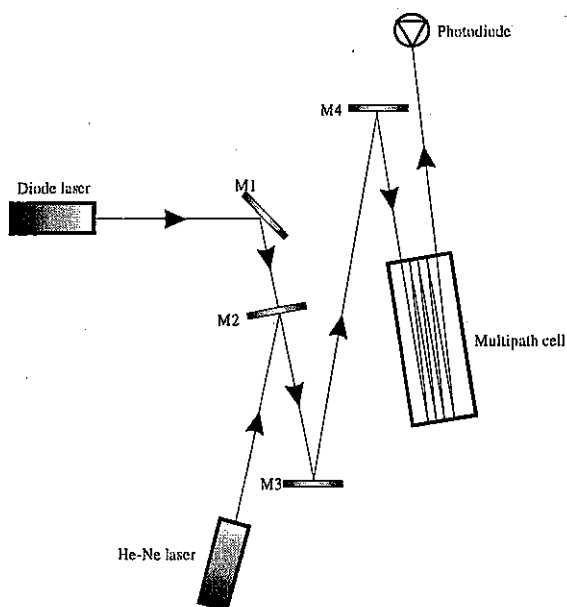


Figure 10: A tuneable diode laser is used as the probe beam. The mirror M2 is transparent for the probe beam because the beam is IR. To align the probe beam a He-Ne laser is used. The beams are combined at M2, which is reflective for the visible beam. After the cell a photo diode is used as a detector.

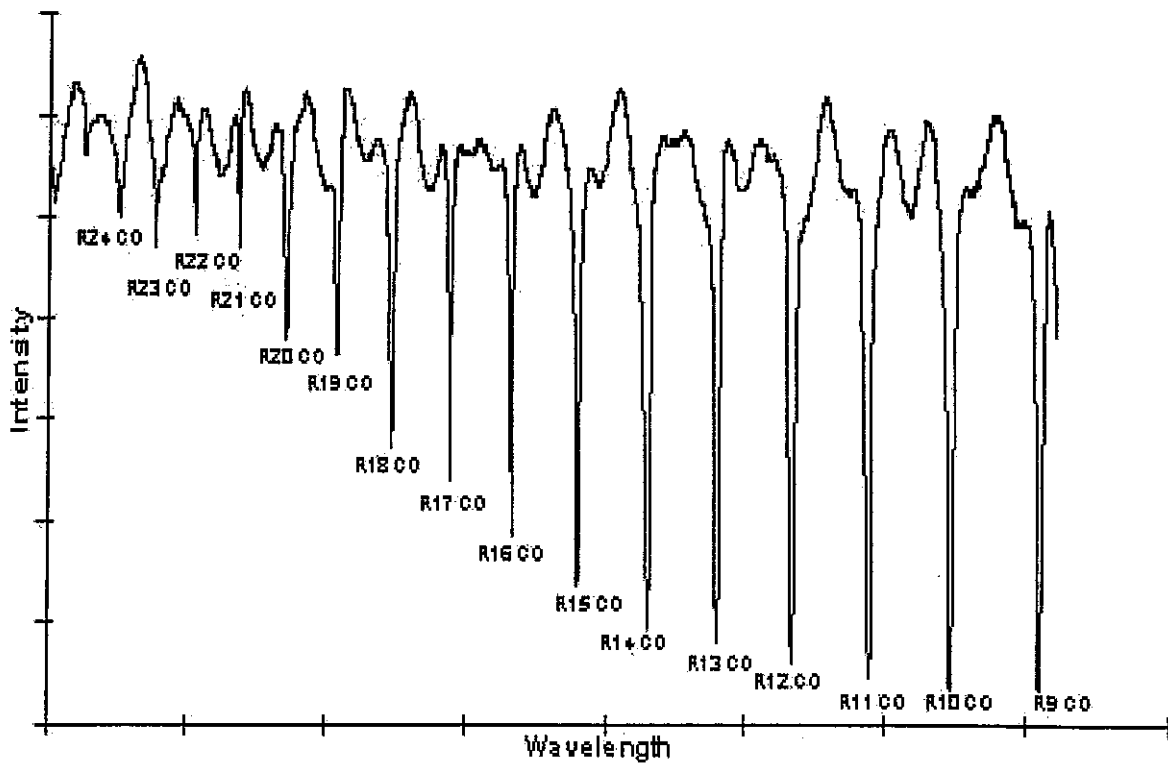
A tuneable diode laser is used as the probe beam. Since the probe beam is in the infrared, a He-Ne laser is used to align the probe beam into the multipath cell. After the multipath cell a photo diode is used as a detector.

### 4.2 Results

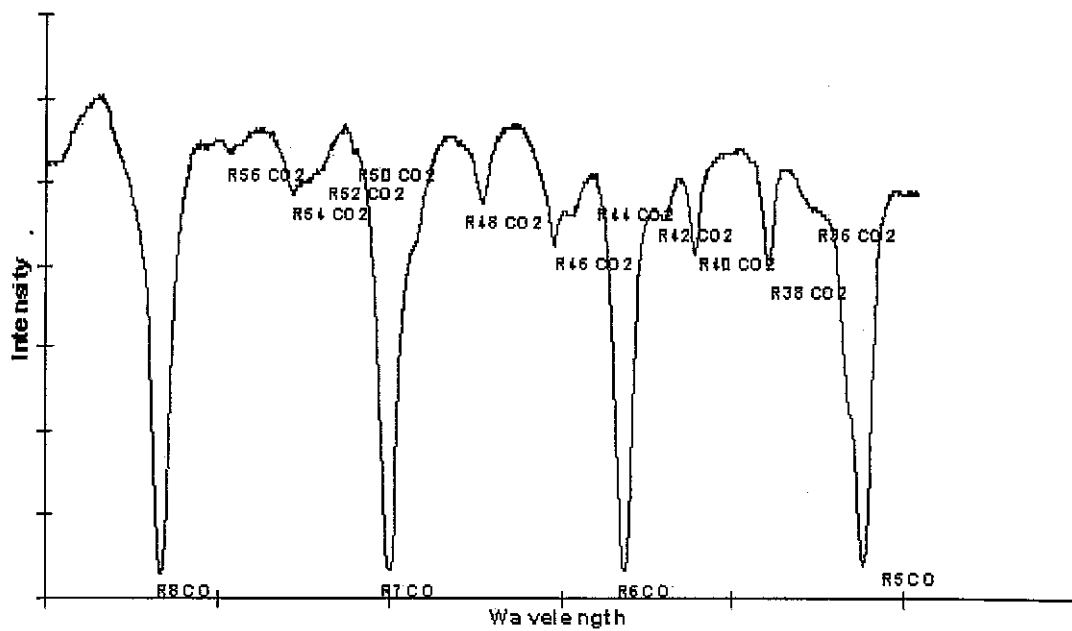
The detector signal was plotted versus time in a computer. From references [Henningsen 1999, Burch 1967, Toth 1969, Chedin 1979, Picqué 1997, HITRAN and Maillard 1980], the positions of some absorption lines were known and the sweep velocity of the tuneable laser for a short measurement time could be calculated.

Some of the spectra obtained at 1 atmosphere total pressure, with a mixture of 40 % CO and 60 % CO<sub>2</sub> can be seen in figure 11.

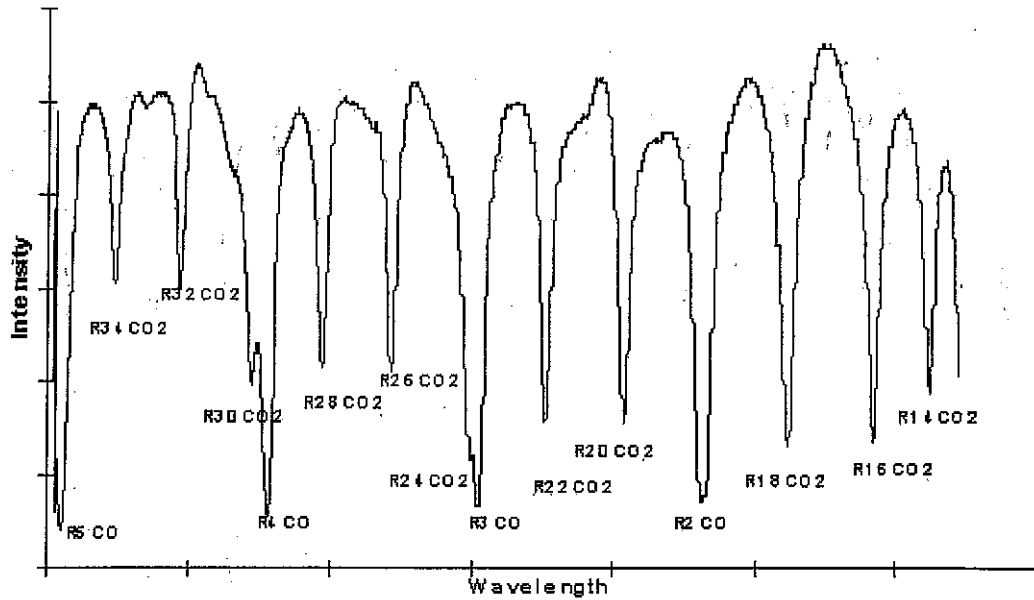
R24 CO at 1559.56nm to R9 CO at 1566.83nm



R8 CO at 1567.32nm to R5 CO at 1569.53nm



R5 CO at 1569.53nm to R14 CO2 at 1572.33nm



P10 CO2 at 1577.35nm to P22 CO2 at 1580.04nm

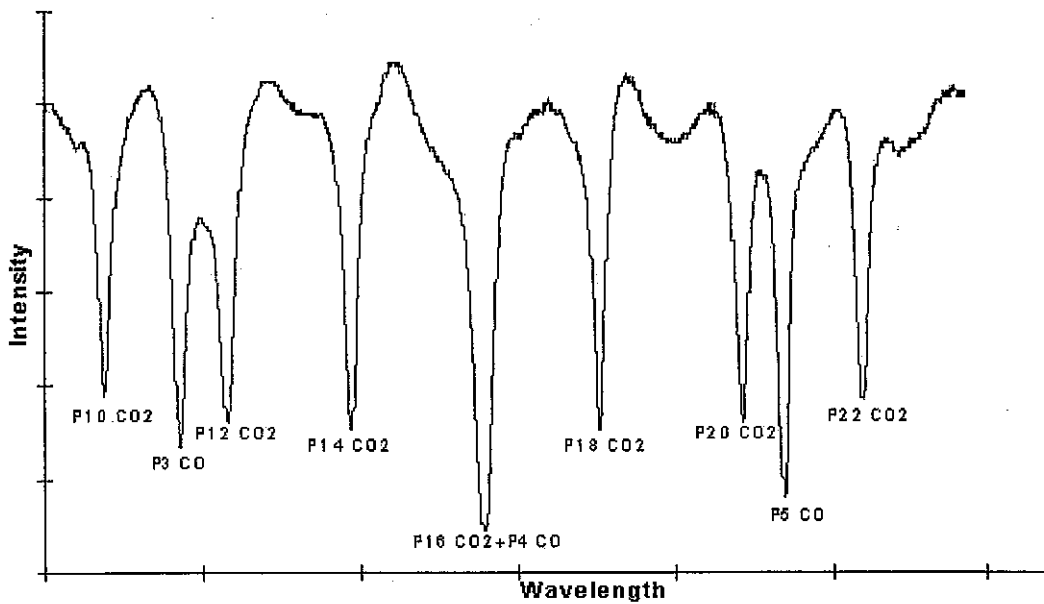


Figure 11: Some of the spectra obtained. The spectra are arranged up and down according to wavelength. The spectra at the top show the characteristic carbon monoxide profile. All spectra are measured at one atmosphere pressure.

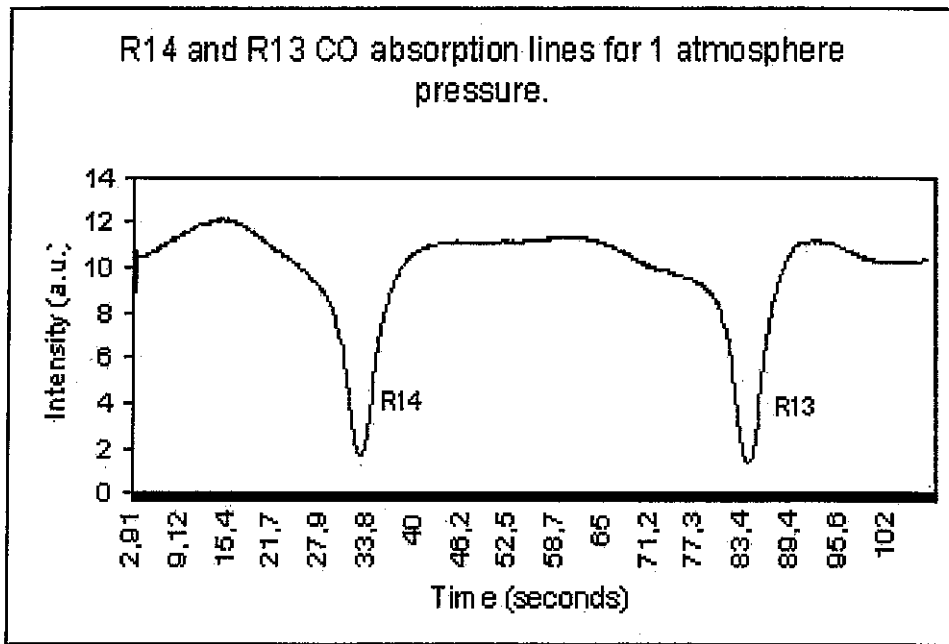


Figure 12: Intensity versus time at one atmosphere pressure.

The data were recorded as intensity versus time in a PC computer.

The first minima (e.g. the R14-line) occur at  $t_1$  and the second minima (e.g. the R13-line) occur at  $t_2$ . This gives a time difference

$$\Delta t = t_2 - t_1.$$

From the references mentioned above we know that the R14 absorption line lies at  $\lambda_1$  and R13 at  $\lambda_2$ . This gives a wavelength difference

$$\Delta \lambda = \lambda_2 - \lambda_1.$$

Assuming that the sweep velocity of the laser was constant during the measurement time a sweep velocity can be calculated

$$v_{laser} = \frac{\Delta \lambda}{\Delta t}.$$

Knowing  $v_{laser}$  and the time when the measurement started, time can be translated to wavelength by using  $\lambda = v_{laser} t$ . Wavelength is not the common spectroscopic unit so the x-scale is recalculated to wave numbers in  $\text{cm}^{-1}$ .

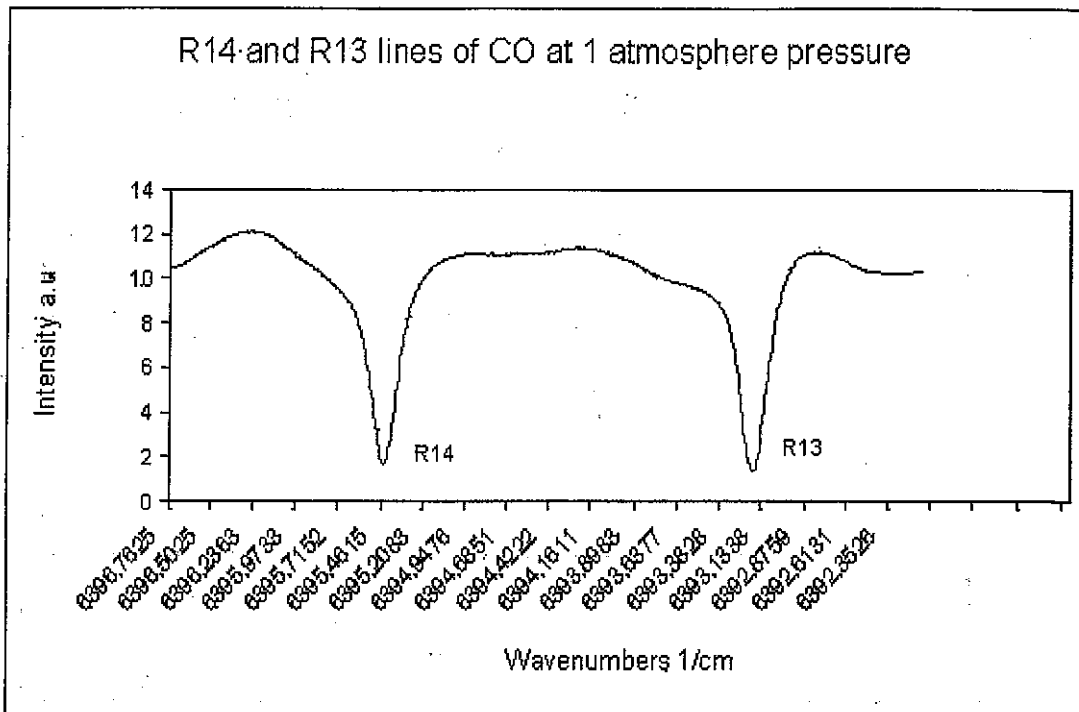


Figure 13: Intensity versus wave numbers at one atmosphere pressure.

When we now have the spectrum the full width at half maximum, FWHM, could be measured. For CO, the R14 line at 1 atmosphere has the FMWH is 6.21 GHz.

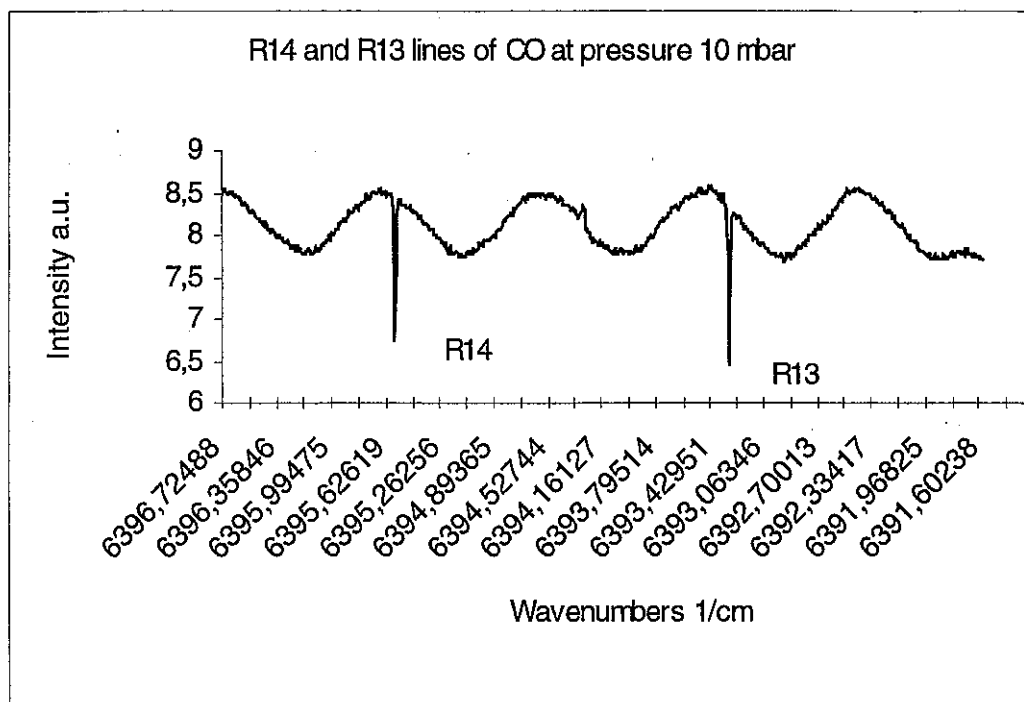


Figure 14: Intensity versus wave numbers at 10-mbar pressure.

The same lines at 10 mbar has a FWHM of 0.45 GHz. Theoretically the Doppler width could be calculated by

$$\delta\omega_D = \frac{\omega_0}{c} \sqrt{(8kT \ln 2 / m)}, \quad [\text{Demtröder 1996}]$$

where  $\omega_0$  is the centre frequency of the absorption line and  $m$  is the mass of the molecule. The Doppler width is independent of the pressure. For the R14 line in carbon monoxide, the Doppler width becomes

$$\delta\nu_D = 0.44 \text{ GHz.}$$

In good agreement with measured line width at 10-mbar (*see* figure 16).

The collision broadening is not as easy as Doppler broadening to calculate. In a close area of the collision broaden line the function can be approximated by the Lorentzian function

$$k(\nu) = \frac{S}{\pi} \left( \frac{\gamma}{(\nu - \nu_0)^2 + \gamma^2} \right), \quad [\text{Burch 1967}]$$

$\nu$  is the frequency,  $S$  is the absorption strength,  $\gamma$  is the half width of the line and  $\nu_0$  is the line centre. The line half width is related to pressure  $p$  by

$$\gamma = \gamma_0 \frac{p}{p_0},$$

with  $p_0$  equal to standard pressure, 1 atmosphere.  $\gamma_0$  can be measured or taken from reference literature. By plotting the Collision induced Lorentzian function with the absorption strength and half width of the line taken from ref. [Burch 1967] the collision broadening for the R14 line at 1 atmosphere of CO becomes

$$\delta\nu_{coll} = 3.83 \text{ GHz}$$

and for the R14 line at 10 mbar

$$\delta\nu_{coll} = 38.3 \text{ MHz.}$$

One can see that the R14 line at 1 atmosphere has a FWHM broader than the Gauss function (Doppler width) and the Lorentzian (Collision width). This could be explained by the fact that the CO sample is not pure. The presence of another gas, in this case 60% CO<sub>2</sub> could broaden the line according to Linnerud [1998]. Figure 15 shows a comparison between the obtained (*lined*) and the theoretically calculated pressure broadening (*dotted*). In the left plot in figure 15 the theoretical data is that only carbon monoxide is used. In the right plot in figure 15 the data is that 0.4 is carbon monoxide with a pressure broadening of 3.8 GHz according to ref. [Burch 1967] and 0.6 is carbon dioxide. Assuming that the pressure broadening is the sum of self broadening and broadening from the carbon dioxide molecule

$$\gamma = 0.4\gamma_{CO} + 0.6\gamma_{CO_2}$$

the broadening contribution from  $\gamma_{CO_2}$  could be determined by fitting the theoretical curve to the measured one by changing  $\gamma_{CO_2}$ . The carbon dioxide parameter becomes  $\gamma_{CO_2} = 7.8$  GHz. The self-broadening is  $0.4 \cdot 3.8$  GHz = 1.52 GHz and the carbon dioxide induced broadening is  $0.6 \cdot 7.8$  GHz = 4.68 GHz. One can see that the carbon dioxide induced broadening is approximately 2 times higher than the self-broadening. That is, collision between carbon monoxide molecules is not as common as collisions between a carbon monoxide molecule and a carbon dioxide molecule. In other words the collision cross section is higher between a carbon monoxide and a carbon dioxide than for a two carbon monoxide molecules.

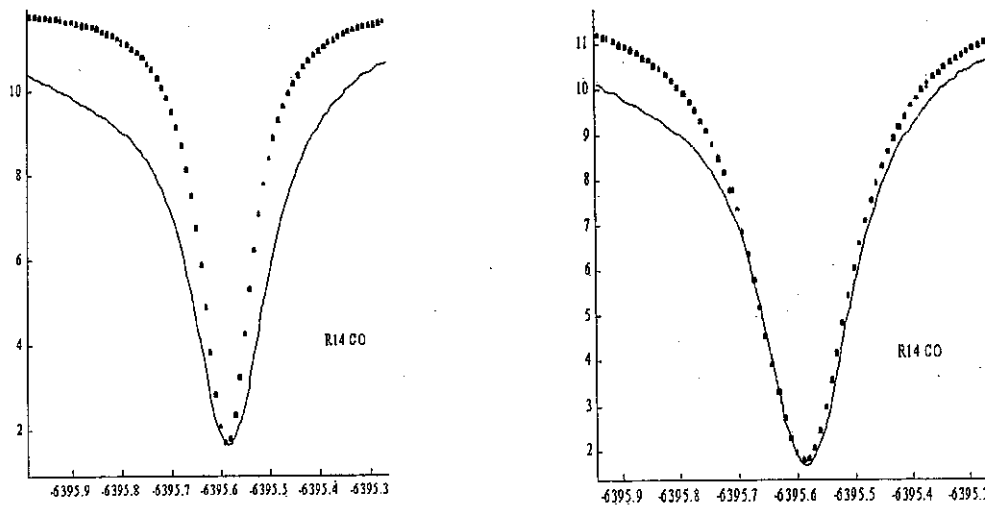


Figure 15: Wave numbers versus intensity. To the left, theoretically collision profile for the R-14 line (*dotted*) compared with obtained spectra. To the right, modified theoretically collision profile for the R-14 line (*dotted*) compared with obtained spectra. The measured spectra are obtained at 1 atmosphere pressure.

For the 10-mbar cases the line is much broader than the collision broadening. But if one compares it with the Doppler broadening one can see that they coincide almost exactly (see figure 16).

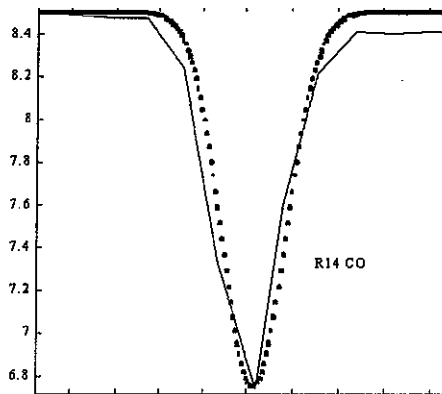


Figure 16: Wavelength versus intensity. Theoretical Doppler profile for the R-14 line (dotted) compared with the obtained spectra at 10-mbar pressures at 1563.61 nm.

As one can see in figure 14, there is a modulation of the background signal. This signal has a period of  $1,088 \text{ cm}^{-1}$ . Low frequency noise is generally from the technical equipment. Assuming that the periodic noise is from the gas cell the noise signal look like a signal from a Fabry-Perot interferometer with a free spectral range of  $1,088 \text{ cm}^{-1}$ .

$$\Delta\nu_{FSR} = \frac{c}{2nd},$$

where  $n$  is the refractive index and  $d$  the thickness of the material. The only thing that could give FSR of  $1,088 \text{ cm}^{-1}$  is the quartz window of the cell. Using FSR of  $1,088 \text{ cm}^{-1}$  and the refractive index for quartz,  $n = 1.5533$ , and solving for the thickness,  $d$  becomes 3.5 mm which is very near the true thickness.

In Appendix B a sine wave is fitted to the background signal. If the fit coincides with the measured data (figure A1), this is proof that the laser works well, without any drifts and with constant velocity. As can be seen there are deviations. This indicates that the laser scan is non-linear.

## 5 Optical or Sub-mm Spectroscopy?

### 5.1 Broadening and Spectral Resolution

The Doppler broadening is proportional to the frequency of the absorption line according to

$$\delta\nu_D = 7.16 \cdot 10^{-7} \nu \sqrt{\frac{T}{M}},$$

where  $M$  is the mass of the molecule expressed in  $u$ . For the R14 line at 191.7 THz in carbon monoxide the Doppler broadening becomes 0.44 GHz. If one now compares this with spectroscopy in the sub-mm region, the Doppler broadening should become less. As an example we can look at the  $1 \leftarrow 0$  transition. The transition has the centre frequency at 115.271 GHz [Winnewisser 1997], this gives a Doppler broadening of 0.267 MHz which is more than a factor  $10^3$  less than for the R14 line. For sufficient low pressures, where the Doppler broadening becomes the limiting factor, the spectral resolution is better in the microwave area.

If one uses Doppler free spectroscopic techniques (Saturation Spectroscopy [Demtröder 1981]), the line width is no longer limited by Doppler Broadening. Here it is the equipment used or the collision line width that determines the resolution.

### 5.2 Absorption Strength

One can also compare sub-mm spectroscopy with optical spectroscopy in terms of the absorption sensitivity. One factor, which determines this, is the amount of absorption, which is  $e^{-\alpha L}$ , since the intensity of the light in an absorption cell decreases as  $e^{-\alpha L}$  where  $\alpha$  is the absorption coefficient and  $L$  is the cell length. This in turn depends on the absorption strength per molecule and the number of molecules. A second determining factor is the (technical) signal-to-noise ratio, associated with the source of electromagnetic radiation or the detector used in the spectroscopy [section 3.3] In [Ye 1997] the absorption sensitivity for different molecular spectroscopy techniques is listed and discussed. For a direct absorption measurement the absorption sensitivity, normalised with  $L=1$ , can be as high as  $10^{-8}$ . For a new technique, NICE-OHMS (Noise Immune Cavity Enhanced Optical Heterodyne Molecular Spectroscopy), sensitivity of  $5.2 \cdot 10^{-13}$  has been reached with a signal to noise ratio of 7700. With this sensitivity it is possible to detect a single atom in  $1 \text{ cm}^3$  volume.

From [Hure 1993] the oscillator strength for an electric dipole transition can be calculated with

$$f_{v'',J''}^{v',J'} = \frac{8\pi^2 m_e}{3h^2 e^2} \frac{E_{v',J'} - E_{v'',J''}}{2J''+1} S_{J''} |D_{v'',J''}^{v',J'}|^2, \quad (5)$$

where  $E_{v',J'} - E_{v'',J''} = \hbar\omega_0$ ,  $\omega_0$  is the centre frequency of the transition,  $J''$  is the lower energy level,  $m_e$  is the electron mass,  $e$  is the electron charge, and  $D_{v'',J''}^{v',J'}$  is the dipole moment.

In the near infrared, the selection rules are  $\Delta J = \pm 1$  and

$$\text{For the R-branch } (\Delta J = +1) \quad S_{J''}^{J'} = J'' + 1$$

$$\text{For the P-branch } (\Delta J = -1) \quad S_{J''}^{J'} = J'' - 1.$$

For the R14 transition in CO, Toth, Hunt and Plyler [1969] quote a dipole moment (squared) of  $D^2 = 0,18 \text{ debye}^2$  (1 Debye =  $3,3356 \cdot 10^{-30} \text{ Cm}$ ). This leads from equation 5 to oscillator strength  $f = 2,9 \cdot 10^{-10}$ .

For the corresponding mm-wave absorption sensitivity, Winnewisser [1997] reached a signal to noise ratio of 15 in their sub-Doppler measurement of the microwave transition  $J = 4 \leftarrow 3$  in carbon monoxide. Further on they had measured the dipole moment in the transition to 0,1 Debye. From this one can calculate the oscillator strength, using equation 5 as  $f = 9,7 \cdot 10^{-9}$ .

The corresponding line intensity, given by

$$S = \frac{\pi \cdot e^2}{m_e \cdot c} f,$$

For the R14 transition in CO:  $S = 0,085 \cdot 10^{-24} \text{ m} \cdot \text{molec}^{-1}$  or  $2,1 \text{ m}^2 \cdot \text{atm}^{-1}$ .

For the mm-transition  $J = 4 \leftarrow 3$  in CO:  $S = 2,9 \cdot 10^{-24} \text{ m} \cdot \text{molec}^{-1}$  or  $77 \text{ m}^2 \cdot \text{atm}^{-1}$ .

To calculate the absorption sensitivity,  $e^{-\alpha L}$ , one needs to know  $\alpha$ . In Appendix A, the connection between  $\alpha$  and  $S$  can be seen. With an integrated value of  $\alpha$  over the line shape (eqn. A3) and with  $L=1 \text{ m}$ , the absorption sensitivity.

For the R14 transition in CO:  $e^{-\alpha L} = 0,12$ .

For the mm-transition  $J = 4 \leftarrow 3$  in CO:  $e^{-\alpha L} = 10^{-31}$ .

This implies that the absorption sensitivity is much higher in the microwave region than in the optical region. In many cases however the signal-to-noise ratio, associated with the source of electromagnetic radiation or the detector used in the spectroscopy, will limit the actual sensitivity. Semiconductor lasers have in general appreciably less intensity noise than sub-mm sources.

### 5.3 Water and Other Limiting Effects

When it comes to compare two different spectroscopic methods it is not only about resolution and detection sensitivity and other technical effects. To be able to perform absorption spectroscopy outside a laboratory, no matter which technique used, there is other limiting effects. When it comes to microwave spectroscopy water is a big problem. Water is a very common molecule in the atmosphere and absorbs strongly in the microwave region. Yasmin [1990] shows this, *see* figure 17. This makes it hard to obtain spectra of carbon monoxide in situations without vacuum chambers.

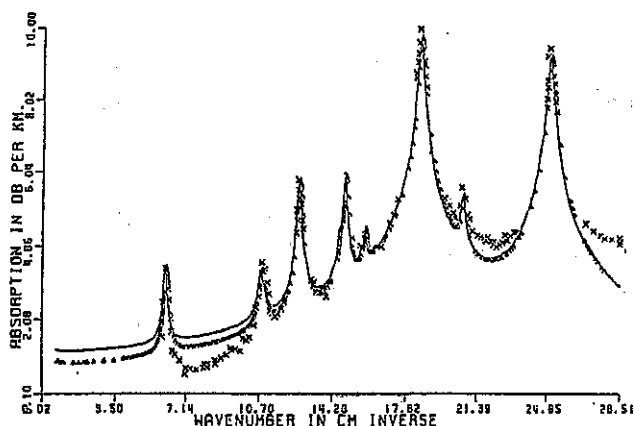


Figure 17: Absorption spectrum of water. The  $J = 4 \leftarrow 3$  transition in carbon monoxide absorbs around  $15.37\text{cm}^{-1}$ . Figure is taken from K. Yasmin [1990].

Picqué [1997] shows that the problem is much less in the optical region, *see* figure 18. As shown in the practical work, carbon dioxide ( $3\nu$ ) absorbs about the same frequencies as carbon dioxide, but it is mostly just the P-branch that is effected. If one has a pure sample of carbon monoxide in a multipath cell, one can obtain pure spectra because the weak absorption from carbon dioxide outside the cell will not effect the measurement.

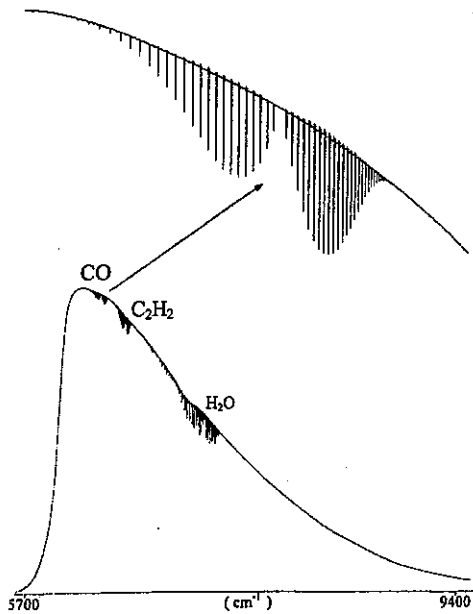


Figure 18: The spectrum of 3-0 band of carbon monoxide. Figure taken from Picqué [1997].

## 6 Conclusion and Future Work

Which of the two methods, laser spectroscopy or microwave spectroscopy, is the best? Of course it depends on what the purpose of the measurement is.

For detection of trace gases, direct laser absorption techniques is the fastest and easiest way. When more sensitive measurements are required a laser modulation technique could be acquired. For detection of species in a mixture or determination of concentration laser spectroscopy offers a simple and relative cheap technique. To use sub-mm spectroscopy in order to detect gases is not to recommend. The microwave absorption spectroscopy requires a lot more complex instruments than laser spectroscopy and cannot be used in detection of non-polar molecules. Another problem with microwave spectroscopy is that gases like  $H_2O$  have a very strong absorption in this region. The measurements can only be performed in windows where this molecule does not absorb. For detection of low concentration or weak absorption the NICE-OHMS offer a very sensitive measurement technique [Ishibashi 1999].

For detection of gas molecules in other planets atmospheres microwave spectroscopy is the one to use. Stars offer a good source of microwave radiation. Water molecule in the earth atmosphere is a problem. Using windows in the water molecule absorption spectra and placing the detector on high ground can reduce this problem. In order to obtain accurate spectra, absorption lines must be decided with high spectral resolution in laboratories.

In the experimental part of this work, a mixture of carbon monoxide and carbon dioxide was used in an absorption spectroscopy experiment. For relatively low pressures the results agree with Doppler theory and could be treated as pure carbon monoxide. At higher pressure, the collision broadening was the dominant broadening effect, and the fact that the gas was a mixture has to be taken into count. The line broadening became broader for the mixture than the theory predicted it should be for a pure carbon monoxide. From literature this could be explained that some gases broaden the line width and carbon dioxide is one of those gases.

To continue this work, sub-mm measurements of carbon monoxide should be performed. A task that has not been done before is to decide the rotational levels in the  $3\nu$  band of carbon monoxide. This could be done with optical pumping with a diode laser and at the same time use microwave spectroscopy of the sample. The rotational transition in the ground state is well known [Mäder 1996] and this could be compensated for.

## References

- C. N. Banwell, *Fundamentals of Molecular Spectroscopy*, (1972).
- S. P. Belov, F. Lewen, Th. Klaus, G. Winnewissen, *Journal of Molecular Spectroscopy* **174**, 606-612 (1995).
- D. E. Burch, D. A. Gryvnak, *Journal of Chemical Physics* **47**, No 12 (1967).
- A. Chedin, *Journal of Molecular Spectroscopy* **76**, 430-491 (1979).
- W. Demtröder, *Laser Spectroscopy*, Springer Verlag (1981).
- W. Demtröder, *Laser Spectroscopy*, Springer Verlag (1996).
- J. Henningsen, H. Simonsen, T. Mogelberg, E. Trudso, *Journal of Molecular Spectroscopy* **193**, 354-362, (1999).
- HITRAN molecular spectroscopic database.
- J. M. Hure, E. Roueff, *Journal of Molecular Spectroscopy* **160**, 335-344 (1993).
- C. Ishibashi, H. Sasada, *Journal of Molecular Spectroscopy* **200**, 147-149 (2000).
- G. De Lange, Quantum Limited Heterodyne Detection of 400-840 GHz Radiation with Superconducting Nb Tunnel Junctions, *Rijksuniversiteit Groningen*, (1994).
- I. Linnerud, P. Kaspersen, T. Jager, *Applied Physics* **B67**, 297-305 (1998).
- J. P. Maillard, M. Cuisenier, Ph. Arcas, E. Arie', C. Amiot, *Canadian Journal of Physics*, **Vol. 58**, 1560-1569, (1980).
- H. Mäder, A. Guarnieri, J. Doose, N. Nissen, V. N. Markov, A. M. Shtanyuk, A. F. Andrianov, V. N. Shanin, A. F. Krupnov, *Journal of Molecular Spectroscopy* **180**, 183-187, (1996).
- N. Picqué, G. Guelachvili, *Journal of Molecular Spectroscopy* **185**, 244-248, (1997).
- R. A. Toth, R. H. Hunt, E. K. Plyler, *Journal of Molecular Spectroscopy* **32**, 85-96 (1969).
- G. Winnewisser, S. Belov, Th. Klaus, R. Scieder, *Journal of Molecular Spectroscopy* **184**, 468-472, (1997).
- K. Yasmin, R. L. Armstrong, *Applied Optics* vol. 29, No. 13, 1979-1983, (1990).
- J. Ye, L. Ma, J. Hall, *Journal of Optical Society of America B*, **Vol. 15**, No. 1, (1998).
- X. Zhu, D. T. Cassidy, *Journal of Optical Society of America B***14**, (1997).

# APPENDICES

## A. Concentration and Signal to Noise Ratio

When it comes to signal to noise ratio, it is of course dependent of the concentration of the species in the measurement.

For a single species of concentration  $C$  in a no absorbing buffer gas, at a total pressure  $p$  and temperature  $T$ , the absorbing coefficient of a given line is

$$\alpha(\nu - \nu_0) = SN_a g(\nu - \nu_0), \quad (\text{A1})$$

where  $\alpha$  is the logarithmic absorption coefficient as determined from Beers law in a linear absorption measurement.

$$I(x) = I(0)e^{-\alpha x},$$

$S$  is the line strength of the absorption line,  $N_a$  is the number density of the absorption molecules, and  $g(\nu - \nu_0)$  is the area normalized line shape function centred at frequency  $\nu_0$ , i.e.,

$$\int_{-\infty}^{\infty} g(\nu - \nu_0) d\nu = 1.$$

The number density can be expressed as

$$N_a = C \frac{p}{kT},$$

where  $k$  is the Boltzmann constant. By measuring  $\alpha(\nu - \nu_0)$  in an absorption cell of length  $L$ , we find a transmitted intensity

$$I(L) = I(0)e^{-\alpha L},$$

and hence the absorption coefficient

$$\alpha(\nu - \nu_0) = -\frac{1}{L} \ln \frac{I(L)}{I(0)}. \quad (\text{A2})$$

Integrating (A1) over the line, we obtain

$$\int_{-\infty}^{\infty} \alpha(\nu - \nu_0) d\nu = SN_a = SC \frac{P}{kT}. \quad (\text{A3})$$

$S$  can be determined by performing the measurement on the pure species where  $C=1$ . Determining  $\alpha$  from equation (A2) we then obtain the concentration of the species in the mixture from equation (A3). According to the procedure outlined above, the result will be independent of the functional form of the line shape function  $g(\nu - \nu_0)$ . However, if the absorption measurement is not carried out over a wide enough range that the absorbance is negligible at the ends of the integration interval, or if there is interference from neighbouring lines, then information about the line shape is required [Henningesen 1999].

## B. Fit to Etalon Fringes

One way of determining the linearity of the spectral scan of the tuneable laser used is to use the periodic background signal (section 4.2, figure 14) interpreted as arising from interference in the windows of the absorption cell.

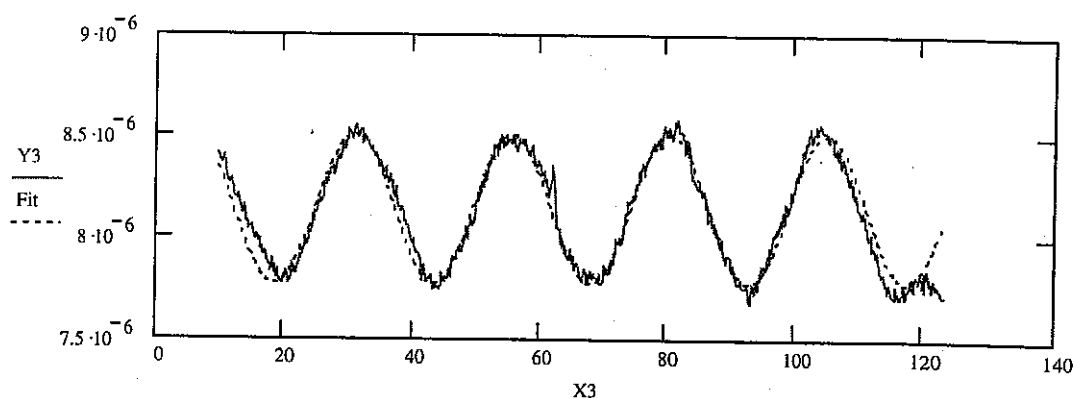


Figure A1: The measured data without the absorption lines, Y3. Fitted function, Fit.

A least-square fit to the experimental data (full line in figure A1, where the molecular signals have been removed) is made of a sinusoidal function

$$I(x) = A_1 \cdot \sin(A_2 \cdot x) + A_3 \quad (\text{A4})$$

of the intensity  $I$  as a function of laser scan,  $x$ . The best fit (dashed line in figure A1) was found to have the parameters:

$$\begin{aligned} A_1 &= -3,69(4) \times 10^{-7} \\ A_2 &= -0,2537(1) \\ A_3 &= 8,133(3) \times 10^{-8} \end{aligned}$$

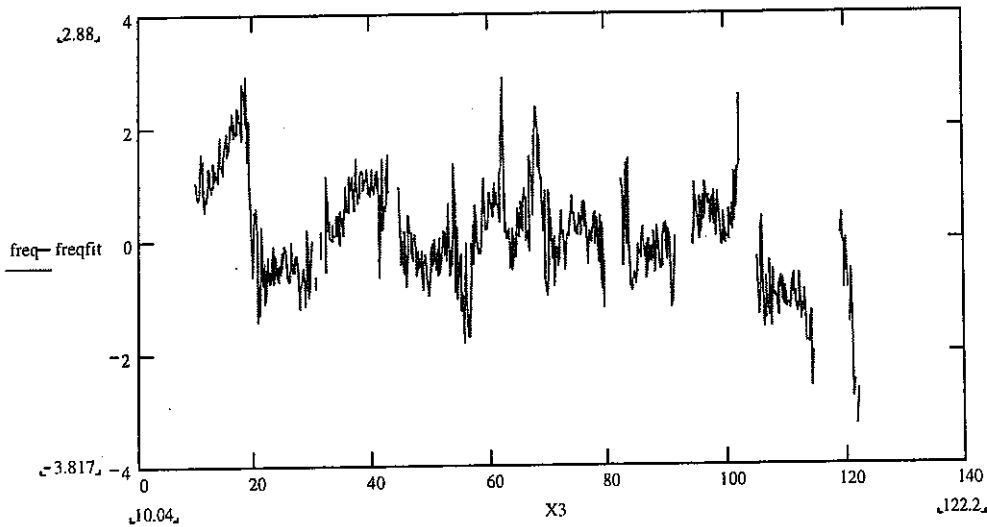


Figure A2: The measured data minus the fitted function.

In order to evaluate the non-linearity of the laser scan, eqn. A4 is inverted to find laser frequency (“x”) as a function of both the experimental and fitted intensities “I” across the scan, using the parameters of the fit.

$$x = \frac{1}{A_2} \cdot \text{asin}\left(\frac{I(x) - A_3}{A_1}\right)$$

Figure A2 shows the difference between these estimates of the frequency. An approximate indication of the actual wave number (x) scale of about 1 GHz/unit is given by the observation of known interval between the CO absorption lines R13 and R14 (figure 14). Deviations from linearity in the laser scan can thus be seen to be on the order of a few hundred MHz, and at most a GHz. This non-linearity may well explain at least part of the observed asymmetry of the collision-broadened lines at 1 atmosphere pressure (figure 12).